Wind and Structures, Vol. 11, No. 4 (2008) 275-289
DOI: http://dx.doi.org/10.12989/was.2008.11.4.275

Systematic influence of different building spacing, height and layout on mean wind and turbulent characteristics within and over urban building arrays

Dehai Jiang, Weimei Jiang*, Hongnian Liu and Jianning Sun

Department of Atmospheric Sciences, Nanjing University, Nanjing, 210093, China

(Received November 22, 2007, Accepted June 17, 2008)

Abstract. Large eddy simulations have been performed within and over different types of urban building arrays. This paper adopted three dimensionless parameters, building frontal area density (λ_f), the variation degree of building height (σ_h), and the staggered degree of building range (r_s), to study the systematic influence of building spacing, height and layout on wind and turbulent characteristics. The following results have been achieved: (1) As λ_f decrease from 0.25 to 0.18, the mean flow patterns transfer from "skimming" flow to "wake interference" flow, and as λ_f decrease from 0.06 to 0.04, the mean flow patterns transfer from "wake interference" flow to "isolated roughness" flow. With increasing σ_h, wind velocity within arrays increases, and the vortexes in front of low buildings would break, even disappear, whereas the vortexes in front of tall buildings would strengthen and expand. Tall buildings have greater disturbance on wind than low buildings do. (2) All the wind velocity profiles and the upstream profile converge at the height of 2.5H approximately. The decay of wind velocity within the building canopy was in positive correlation with λ_f and r_s. If the height of building arrays is variable, Macdonald's wind velocity model should be modified through introducing σ_h, because wind velocity decreases at the upper layers of the canopy and increases at the lower layers of the canopy. (3) The maximum of turbulence kinetic energy (TKE) always locates at 1.2 times as high as the buildings. TKE within the canopy decreases with increasing λ_f and r_s but the maximum of TKE are very close though σ_h varies. (4) Wind velocity profile follows the logarithmic law approximately above the building canopy. The Zero-plane displacement z_d heighten with increasing λ_f, whereas the maximum of and Roughness length z_0 occurs when λ_f is about 0.14. z_d and z_0 heighten linearly with σ_h and r_s, If σ_h is large enough, z_d may become higher than the average height of buildings.

Keywords: large eddy simulation; turbulent flow characteristics; urban building arrays; urban meteorology.

1. Introduction

The urban surface always consists of a large collection of buildings and other obstacles. As this rough surface interacts with the atmospheric flow within and above it, the distribution of mean wind and turbulence can become extremely complicated. Particularly in the huge urban centers, it is difficult to describe the flow and turbulent characteristics accurately because of irregular building geometry and non-uniform building spacing, height and layout. However, it is very important to understand the relationship between the airflow characteristics and the geometrical properties of

* Corresponding Author, E-mail: jwm@nju.edu.cn

urban surface to investigate urban atmospheric problems such as urban meteorology and the dispersion of pollutant in the urban area.

The mean wind and turbulent characteristics within and above urban building arrays have been widely studied these years. Macdonald (2000) presented that the mean velocity obeyed an exponential decay law within urban cube arrays that are not too densely packed by analyzing a set of wind-tunnel data. Macdonald, *et al*. (2002) also used a hydraulic flume to study urban surface layer parameterizations and found that the non-dimensional RMS turbulence components scaled by the local values of the shear stress seemed to be constant in the internal boundary layer above the buildings. Cheng and Castro (2002) made comprehensive laboratory experiments for flow over cube arrays and carefully investigated the spatial averaged wind and turbulent statistics in urban roughness sub-layer and the surface parameterization over urban surface. Hanna, *et al*. (2002) investigated the mean flow and turbulence within simple obstacle arrays by numerical simulations and a hydraulic water flume experiment. In their paper the authors compared the “street canyon” effect between square arrays and staggered arrays. Cheng, *et al*. (2003) used the large eddy simulation (LES) with three different subgrid-scale models and Reynolds-averaged Navier–Stokes (RANS) approaches to deal with a fully-developed turbulent flow over cube arrays and found that the LES with the localized dynamic subgrid-scale model gave a better overall quantitative agreement with the experimental data than RANS. Kanda, *et al*. (2004) investigated the systematic influence of cube density on turbulent flow characteristics by performing numerical experiments and analyzed the turbulent organized structures. Lien, *et al*. (2003, 2005) diagnosed the dispersive stress within and above the building array and the drag coefficient for the aligned cube array by a high-resolution RANS flow model. Coceal, *et al*. (2006) obtained very high time and spatial resolution data by direct numerical simulations of turbulent flow over the regular arrays of urban-like, cubical obstacles. The authors analyzed the turbulent unsteady effects, the mean flow structure and turbulence statistics.

In most above-mentioned researches, the height of the buildings was constant and the arrays were aligned. However, in the actual cities, the height of urban building arrays is always variable and the layout of building arrays is usually staggered. Though Kanda, *et al*. (2004) studied the systematic influence of different cube densities on turbulent flow characteristics, Cheng, *et al*. (2002), Macdonald, *et al*. (2002) and Coceal, *et al*. (2006) compared the difference of turbulent flow between square arrays and staggered arrays, they have not investigated the systematic influence of the variation degree of building height and the staggered degree of building range on airflow and turbulent characteristics in detail.

This paper suggested that most of urban building arrays could be described from three aspects without referring to the shape of buildings. The three aspects are the spacing, height and layout of the building arrays. The main objective of this paper was to study the systematic influence of building spacing, height and layout on the mean flow and turbulent characteristics. This paper focused on (1) the mean wind structure and turbulent characteristics depended on the building spacing, height and layout of the urban building arrays, (2) the similarity law and urban surface parameterization above these urban-like canopies.

2. Computational method

The large eddy simulation (LES) models that are used in this paper are developed by Zhang, *et al*. (2006). They used these models to simulate the flow in an urban block and achieved satisfactory results. The detailed introduction and validation of the LES model could be made reference in their paper.

2.1. Experiment design

Three dimensionless parameters could be used to describe the spacing, height and layout of the urban building arrays. They are building frontal area density (λ_f), the variation degree of building height (σ_h) and the staggered degree of building range (r_s) could be defined as follows:

$$\lambda_f = \frac{d \times H}{L_x \times L_y} \tag{1}$$

$$\sigma_h = \sqrt{\frac{1}{n}\sum_{i=1}^{n}\left(\frac{h_i - H}{H}\right)^2} \tag{2}$$

$$r_s = 2 \times \frac{l}{L} \tag{3}$$

where d is the width of the building, H is the average height of building arrays, L_x, L_y are the streamwise and lateral length of the lot area occupied by a single building, h_i is the height of each building in the arrays, n is the total number of buildings in the arrays, L is the lateral space of adjacent buildings which are in the same row, l is the minimum lateral space of adjacent buildings which are in adjacent rows. The buildings are distributed as shown in Fig. 1.

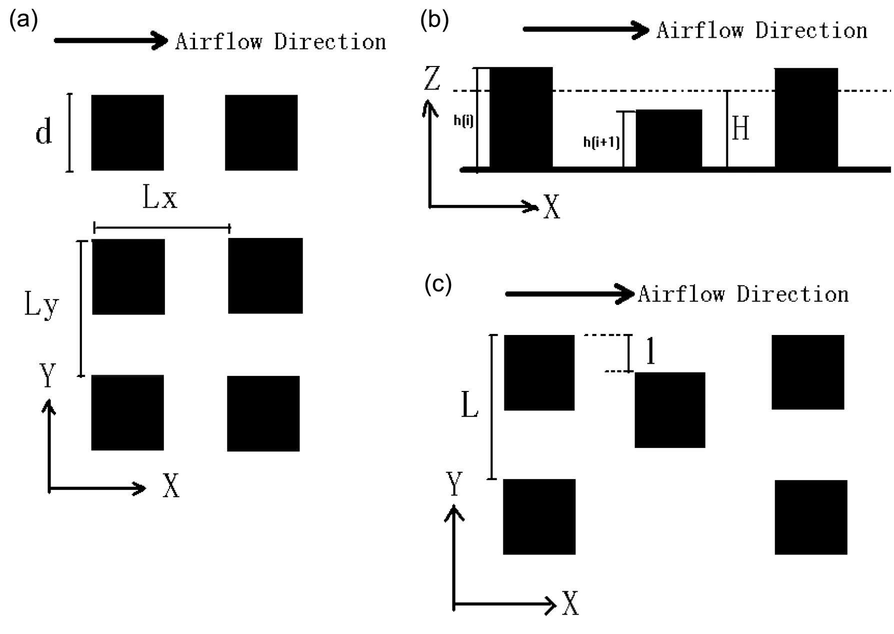

Fig. 1 Distribution of three types of building arrays ((a), (b) and (c) show three kinds of experiment cases in table 1: (a) corresponds to D1-D9, the buildings are all identical cubes with the height 30 m and L_x, L_y changed with different λ_f; (b) corresponds to F0-F5, the horizontal plane of each building are 30 m × 30 m, but the height of the buildings is variable on condition that the average height of building arrays is 30 m; (c) corresponds to S0-S5, the buildings are the same with (a), but the buildings is staggered as l changes)

Table 1 Design of computational condition

Experiment Cases	l_f	s_h	r_s	L_x	L_y	h_{high}	h_{low}	l
D1	0.04	0	0	5H	5H	H	H	0
D2	0.06	0	0	4H	4H	H	H	0
D3	0.09	0	0	3.3H	3.3H	H	H	0
D4	0.11	0	0	3H	3H	H	H	0
D5	0.14	0	0	2.6H	2.6H	H	H	0
D6	0.18	0	0	2.3H	2.3H	H	H	0
D7	0.25	0	0	2H	2H	H	H	0
D8	0.36	0	0	1.6H	1.6H	H	H	0
D9	0.56	0	0	1.3H	1.3H	H	H	0
F0	0.11	0	0	3H	3H	H	H	0
F1	0.11	0.17	0	3H	3H	1.17H	0.83H	0
F2	0.11	0.33	0	3H	3H	1.33H	0.67H	0
F3	0.11	0.5	0	3H	3H	1.5H	0.5H	0
F4	0.11	0.67	0	3H	3H	1.67H	0.33H	0
F5	0.11	0.83	0	3H	3H	1.83H	0.17H	0
S0	0.11	0	0	3H	3H	H	H	0
S1	0.11	0	0.11	3H	3H	H	H	0.17H
S2	0.11	0	0.22	3H	3H	H	H	0.33H
S3	0.11	0	0.44	3H	3H	H	H	0.66H
S4	0.11	0	0.67	3H	3H	H	H	H
S5	0.11	0	1	3H	3H	H	H	1.5H

(λ_f: building frontal area density; σ_h: the variation degree of building height; r_s: the staggered degree of building range; L_x, L_y: longitudinal and lateral length of the lot area occupied by a single building; h_{high}: height of tall building; h_{low}: height of low building; l: minimum lateral space of adjacent buildings which are in adjacent rows)

Table 1 lists the experiment cases of this study. Three series of experiments (D1-D9, F0-F5 and S0-S5) have been done to investigate the influence of various λ_f, σ_h and r_s on the mean wind and turbulent characteristics respectively. The upstream velocity is approximated by the following power-law form:

$$\frac{U(z)}{U_{ref}} = \left(\frac{z}{H}\right)^{0.2} \tag{4}$$

Where $U_{ref} = 5$ m/s is the reference velocity of the upstream flow at $z = H$. The Reynolds number based on the building height H and the reference velocity U_{ref} is almost 10^7. This Reynolds number is high enough for the turbulent flow to be independent of Reynolds number (Snyder, *et al*. 2002, Uehara, *et al*. 2003).

2.2. Domain, grid resolution and time step

It is very important to choose suitable domain, grid resolution and time step because of the large CPU time and memory capacity requirement of large eddy simulations. Kanda, *et al*. (2004)

suggested that a computational streamwise scale of domain is at least an order of magnitude larger than the canopy height, because turbulent organized structures (TOS) are longitudinally an order of magnitude larger than the canopy height and cannot be properly simulated in a small computational domain due to a limitation arising from the cyclic conditions. However, Coceal, *et al*. (2006) thought that the mean flow and turbulence statistics can be captured accurately with even a relatively small domain size, by exploiting the regularity of the geometry with the application of periodic boundary conditions in the horizontal directions. If one were not interested in studying unsteady large-scale organized structures, it would not be necessary to choose large domain. In this paper the authors presented that the spatially averaged results is comparatively depended on grid resolution and should use the higher grid resolution to obtain the better simulation results. The authors adopted H/32 as the grid resolution in their paper. Based on the work of the predecessors, we adopted 4 rows of buildings in the streamwise direction, 3 lines of buildings in the lateral direction and the height of domain was 6H in vertical direction, because the paper did not simulate the large–scale turbulent structures. The computation grid resolution was H/24 and the memory grid resolution was H/6. The grid resolution did not only hold simulation accuracy, but also reduced the memory capacity. The time step was 0.1s. Each simulation lasted for 8 hours to ensure the flow was quasi-steady with fully-developed turbulence. Then we selected the results from the last three hours for the analysis.

2.3. Boundary conditions

Periodic boundary conditions were used for both laterally and streamwise boundaries in order to simulate fully-developed turbulence. The free slip boundary condition was imposed at the top of the domain. No-slip and impermeability boundary conditions were applied at the bottom and on all obstacle surfaces where there were no flow and no scalar flux across the boundary. At all the building boundaries (walls and roofs), standard wall functions were applied for the mean velocities and turbulence quantities at these solid boundaries (Lien, *et al*. 2004).

3. Results and discussion

3.1 Mean flow pattern

Three typical flow regimes ("skimming" flow, "wake interference" flow and "isolated roughness" flow) within the urban canyon are well-known in the literature. Oke, *et al*. (1988), Hunter, *et al*. (1992) and Zhang, *et al*. (2004) discussed the different ratios of H/W and L/H which are the important determining factors of flow regimes (H, the height of building; W, L, the width and length of a canyon). But it is difficult to estimate the value of H, W and L because of the irregular building geometry and non-uniform distribution in real cities. The three mean streamline patterns also appear with the change of λ_f (Kanda, *et al*. 2004). This paper focuses on the transition of flow regimes with the change of λ_f. In all cases, "skimming" flow occurs in D7-D9 (Fig. 2 (a), λ_f is from 0.25 to 0.56), and the street canyon is too narrow to form entire symmetrical vortexes between two adjacent rows of buildings; "wake interference" flow occurs in D3-D6 (Fig. 2 (b), λ_f is from 0.08 to 0.18), the entire double-eddy circulation exists in the street canyon. The vortex cores are located closer towards the leeward wall of the upstream building and the downwind building could disturb the wake flow of the double-eddy circulation and "isolated roughness" flow occurs in D1-D2 (Fig. 2 (c), λ_f is from 0.04 to 0.06), the space between two adjacent rows of buildings is wide enough that

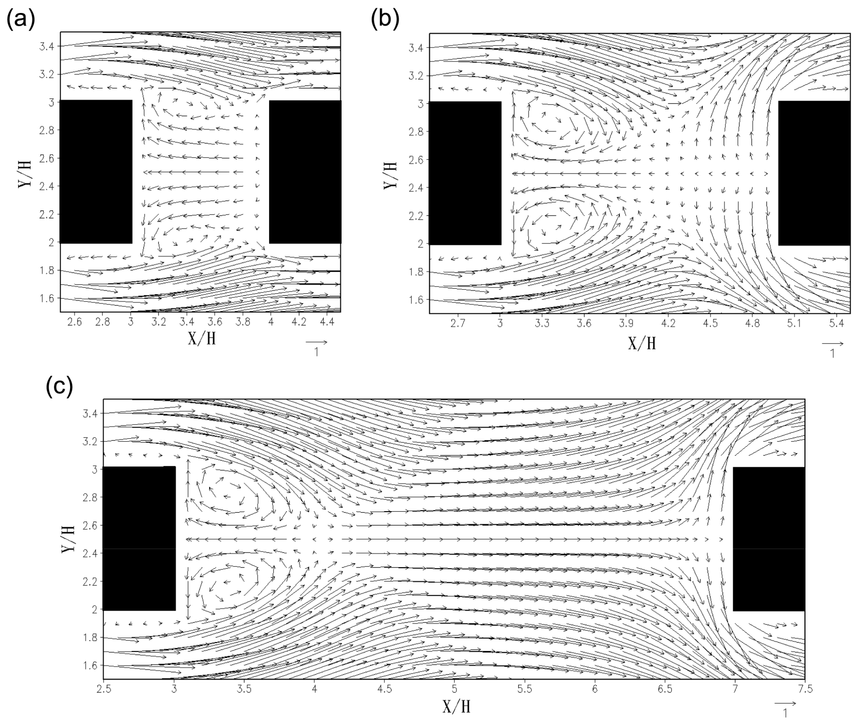

Fig. 2 Mean vector patterns of different λ_f ((a), (b), and (c) are the wind fields in the *x*-*y* plane at $z = 0.1$H for $\lambda_f = 0.25$, 0.11, and 0.04 respectively)

the flow can return to the upwind profile before the leeward building is encountered. The downwind building does not disturb the wake flow of the double-eddy circulation. The simulated results are analogous to the study from Kanda, *et al*. (2004), but the cores of double-eddy circulation are closer to the leeward wall of the upstream building than the results from Kanda. That is because the upstream velocity and the Reynolds number in our experiments are greater than Kanda's.

The vector fields within building arrays of various σ_h are displayed in Fig. 3. As the height of buildings is equal ($\sigma_h = 0$), the clockwise vortexes occur in the street canyon. The shape and size of the vortexes are similar (Fig. 3 (a)). With increasing σ_h, the vortexes in front of the low buildings break, but the vortexes in front of the high buildings strengthen and expand. The downward flow changes into upward flow in front of the low buildings, and the wind velocity within the building arrays increases (Fig. 3 (b)). If σ_h is large enough, the clockwise vortex in front of the low building disappear entirely and the influence of low building on airflow seems to be ignored. The new combined circulation occurs between the high buildings: One clockwise vortex occurs behind the upper layers of leeward wall and another clockwise vortex occurs in front of the lower layers of frontal wall. The flow pattern becomes the typical "wake interference" flow (Fig. 3 (c)).

The mean wind velocity within building arrays of various r_s is shown in Fig. 4. Obviously, as the buildings are aligned, the "street canyon" effect occurs between two lines of adjacent buildings and the wind velocity in the street canyon is very large. The regular double-eddy circulation is distributed behind the buildings. The "low wind velocity" zone exists along the building lines (Fig. 4 (a)). With increasing r_s, the "street canyon" effect decreases and the "low wind velocity" zones

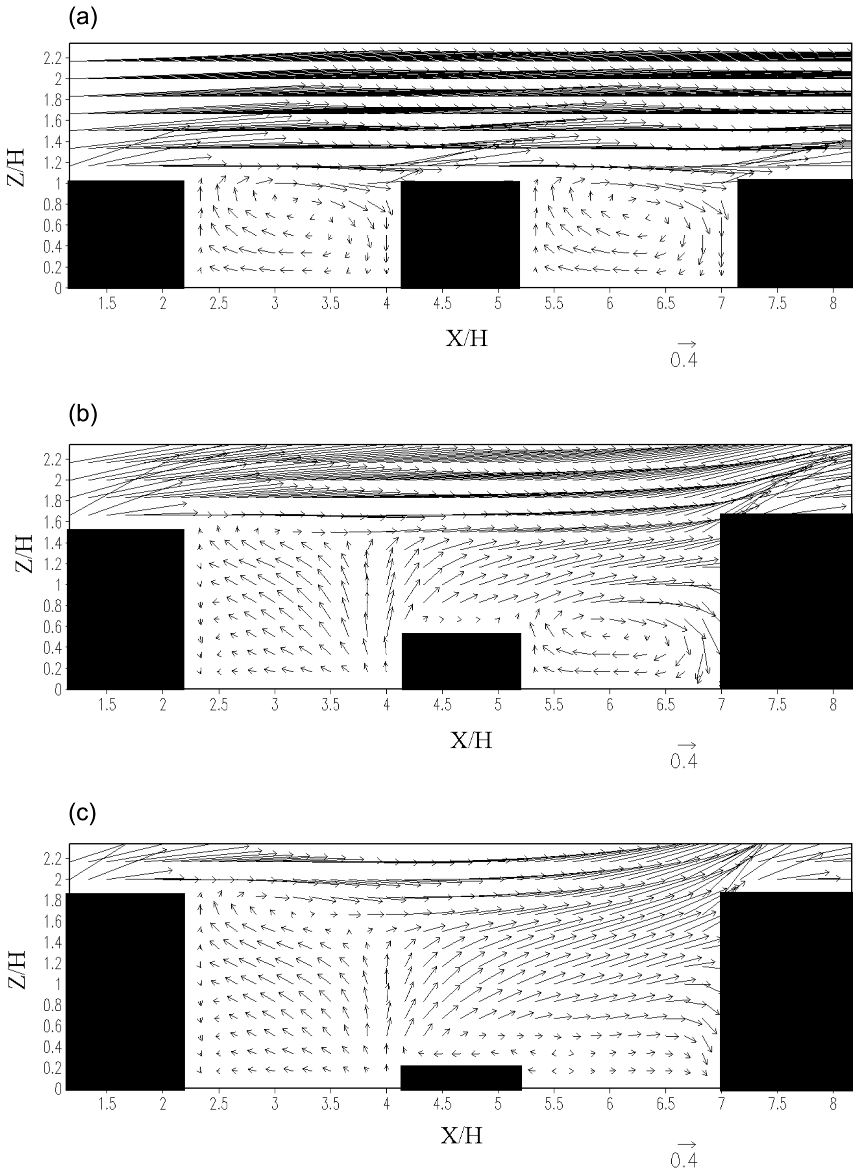

Fig. 3 Mean streamline patterns of various σ_h ((a), (b) and (c) are stream fields in the x-z cross-section at the canyon centre for $\sigma_h = 0$, 0.33 and 0.83 respectively)

are broken (Fig. 4 (b)). If r_s is large enough, the “street canyon” effect would disappear. The wind velocity in building array region becomes low (Fig. 4 (c)).

3.2. Horizontally-averaged mean wind velocity

The horizontally-averaged mean wind velocity profiles $<\bar{u}>$ are displayed in Fig. 5 (The over bar denotes a temporal average, $< >$ represents a horizontal average; the average method could be

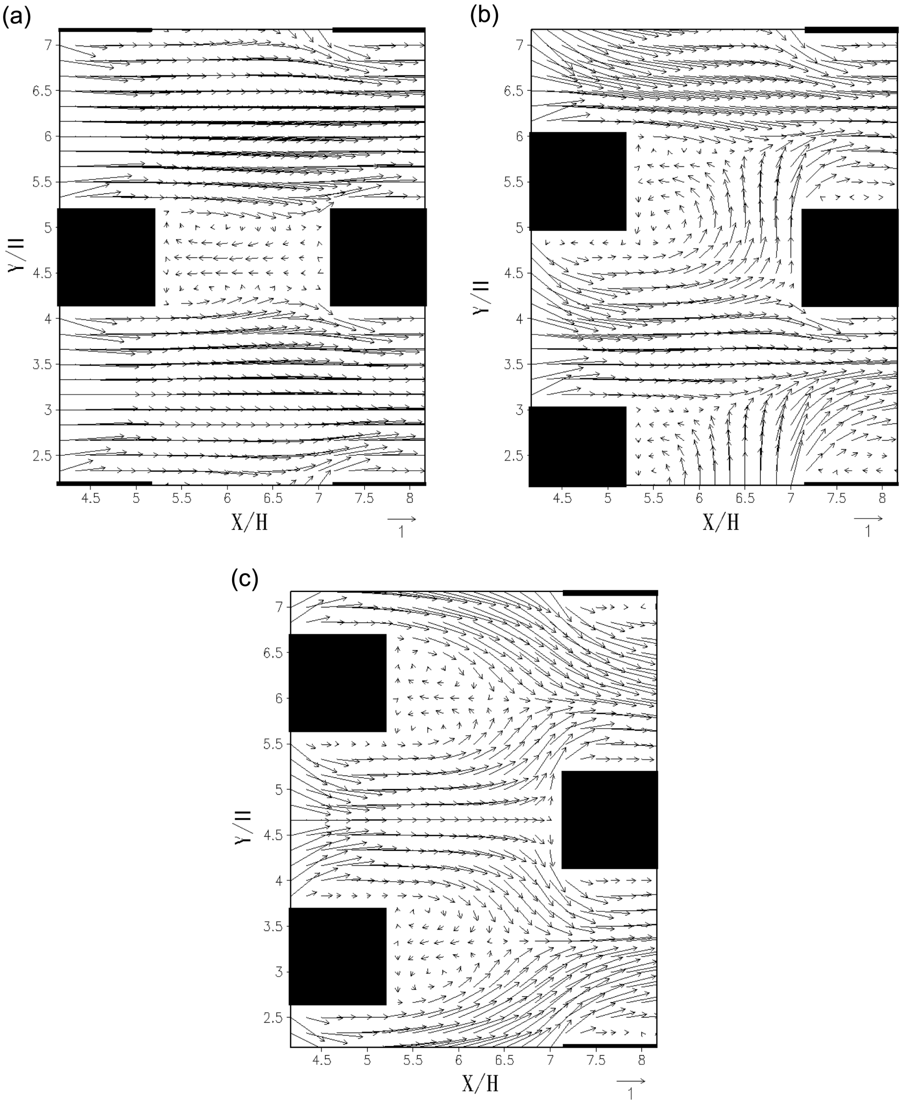

Fig. 4 Mean wind velocity of different r_s ((a), (b), and (c) are mean wind velocity fields in the x-y plane at $z = 0.1$H for $r_s = 0$, 0.22 and 1 respectively)

referred to in the papers of Macdonald, *et al*. (2000) and Kanda, *et al*. (2004).

The influence of λ_f on $<\bar{u}>$ is shown in Fig. 5 (a). The wind velocity decays especially within the building arrays because the buildings drag the flow. The wind velocity profiles are sensitive to λ_f. The larger the λ_f is, the less the wind velocity is within the building canopy, but the wind velocity is in positive correlation with λ_f above the building canopy. All the wind velocity profiles and the upstream profile converge at the height of 2.5H approximately. The influence of σ_h on $<\bar{u}>$ is shown as Fig. 5 (c). The wind velocity profiles depend on σ_h specially. The wind velocity increases with increasing σ_h within the building canopy, whereas it is just the opposite above the building canopy. The reason is that as σ_h increases, the height variation between the buildings becomes

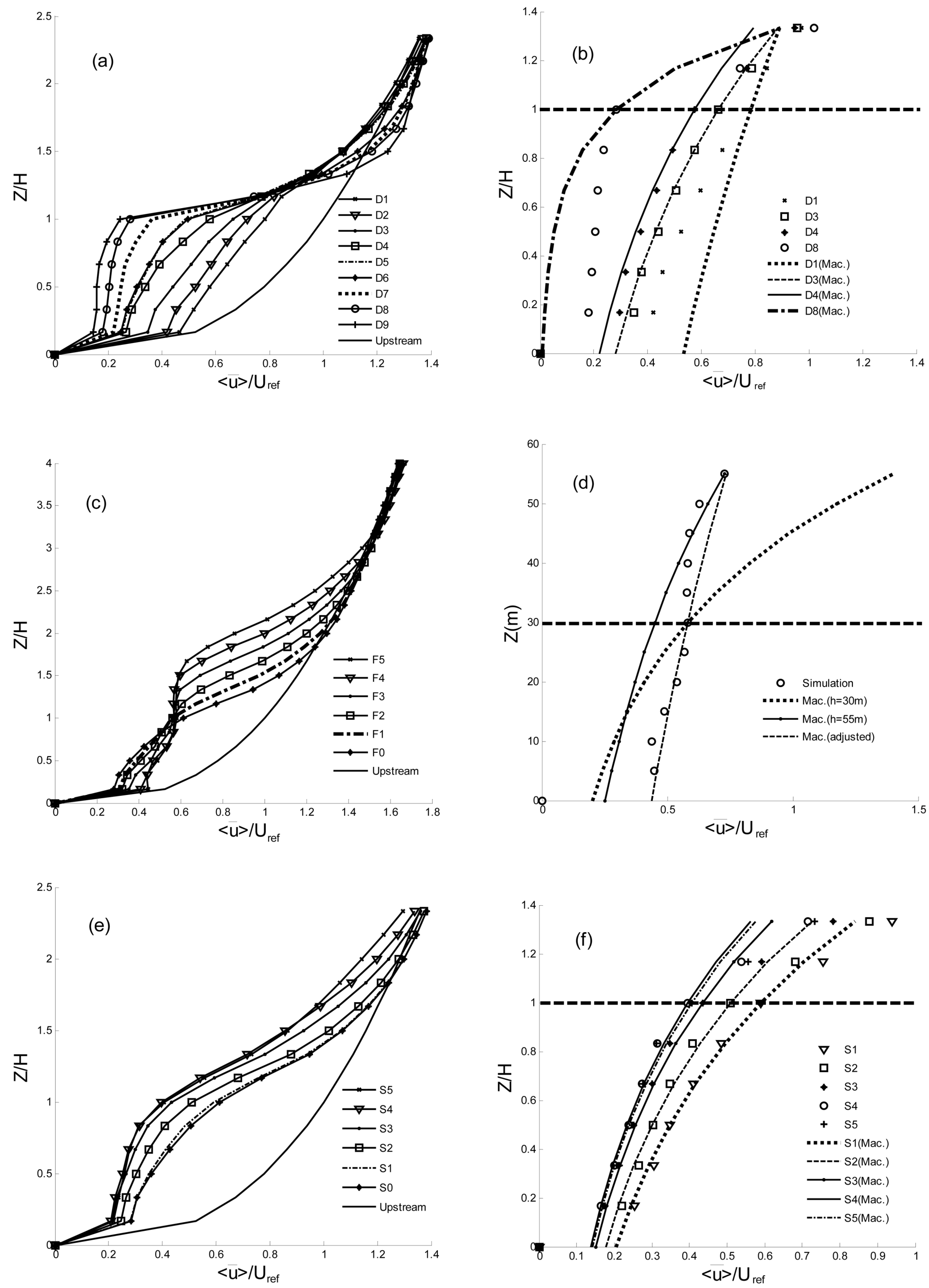

Fig. 5 Horizontally-averaged mean wind velocity profiles for different λ_f, σ_h and r_s

greater. Consequently, the high buildings would drag wind at a higher position, but the drag effect of the lower building would be unobvious. So the larger σ_h is, the smaller the wind velocity is in the upper canopy layers, whereas the larger the wind velocity is in the lower canopy layers. Cheng, *et al*. (2002) considered that the wind velocity decays more significantly in a building array with random height (σ_h is very large) than in a building array with uniform height. Our results support their conclusions. The influence of r_s on $<\bar{u}>$ is shown as Fig. 5(e). The wind velocity profiles are sensitive to r_s too. The decay of wind velocity increases with increasing r_s from the ground to 2.5H on the whole. Cheng, *et al*. (2002) considered that the staggered building arrays drag the airflow more significantly than aligned building array. Our study results accord with their research.

Macdonald, *et al*. (2000) suggested the mean wind velocity obeys an exponential decay law within the urban canopy layer. The authors modified a simple model derived for mean wind speed profiles in vegetative canopy (Cionco 1972) and applied it to study the wind in urban building arrays. The model is as follows:

$$u(z) = u_H \exp\left(a\left(\frac{z}{H} - 1\right)\right) \tag{5}$$

where H is the canopy height, U_H is the wind velocity at canopy height, and a is an attenuation coefficient. The authors found that the attenuation coefficient a = 9.6 λ_f for aligned and staggered arrays of cubes by applying the model to a set of wind-tunnel data. This paper applied Eq. (5) to fit the wind velocity profiles to evaluate the results of our simulation. The simulation results accord with Eq. (5) very well for square and staggered building arrays which are not too densely and sparsely packed (Fig. 5 (b), (f)).

Whereas, whether H is the average height of buildings (short dashed line in Fig. 8 (d)) or the height of higher buildings s(dotted line in Fig. 5 (d)) in the arrays, Eq. (5) can not satisfactorily describe the wind velocity profiles in building arrays of variable height. So σ_h should be considered in Eq. (5). We modified Eq. (5) as follow:

$$u(z) = u_H \exp\left(a_*\left(\frac{z}{H} - 1\right)\right) \tag{6}$$

$$a_* = a \times (1 - \sigma_h) \tag{7}$$

Eq. (6) and Eq. (7) provide a better fit to the wind velocity profiles within building arrays of different σ_h (long dashed line in Fig. 5 (d)) than Eq. (5).

3.3. Horizontally-averaged mean turbulence kinetic energy

Vertical profiles of turbulence kinetic energy, TKE, are displayed in Fig. 6. The TKE profiles of different λ_f are displayed in Fig. 6 (a). Except D1 (the buildings of D1 are very sparse), the maximum of TKE is at 1.2H. The configuration of vertical profiles depends on flow patterns. As the "skimming" flow (λ_f = 0.56-0.25), TKE is very small because the buildings are so dense that the wind velocity is too small. As the "wake interference" flow (λ_f = 0.18-0.08), TKE increases with increasing λ_f within H. As the "isolated roughness" flow (λ_f = 0.06-0.04), the figures of vertical profiles are changed largely. D1 has one inflection points below 0.5H especially. The TKE profiles of different σ_h are shown in Fig. 6 (b). The maximum of TKE locates at 1.2 times as high as the taller building in the arrays and are very close though σ_h varies. The TKE profiles are sensitive to σ_h, TKE reduces with increasing σ_h below the height of the shorter buildings but increases with increasing σ_h above the height of the taller buildings. The TKE profiles of different r_s are shown in Fig. 6 (c). The maximum of k is at 1.2H too. The TKE profiles are sensitive to r_s, TKE decreases

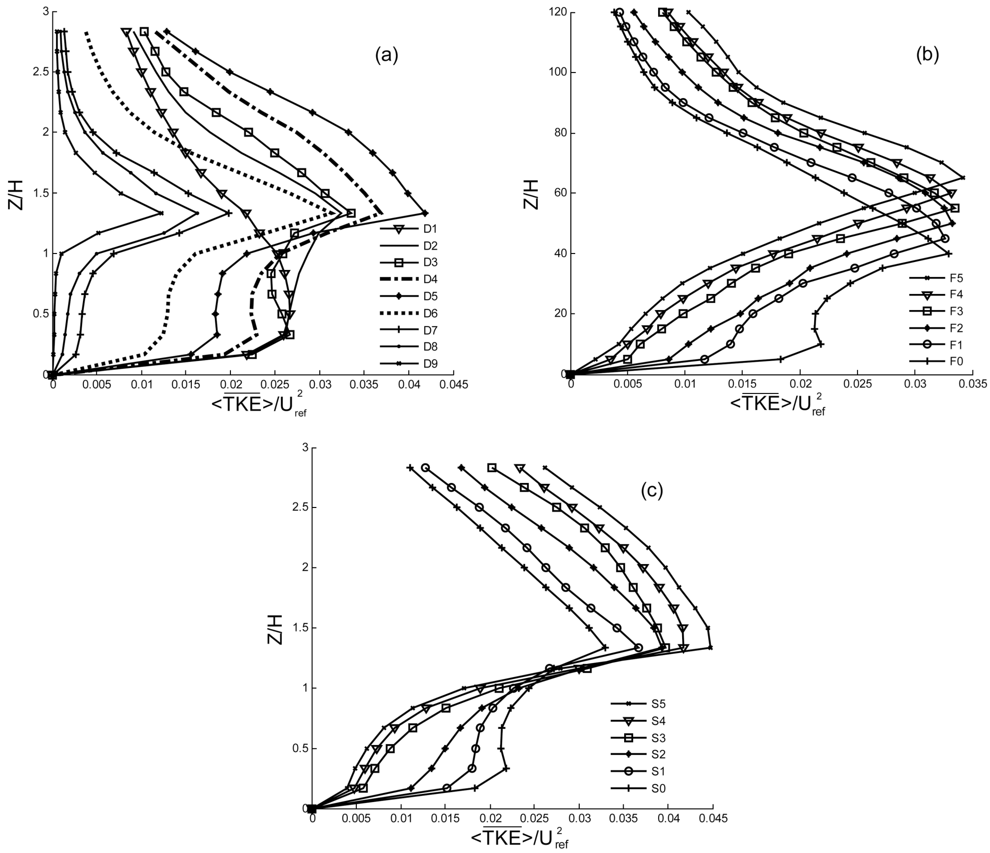

Fig. 6 Horizontally-averaged mean turbulence kinetic energy, TKE, for different λ_f, σ_h and r_s

with increasing r_s below H but increases with increasing r_s above H.

3.4. Urban surface parameters

Raupach (1986) suggested the averaged velocity profile in the roughness sublayer over a plant canopy was not logarithmic. Whereas the research from Cheng indicated that averaged mean velocity profile followed the logarithmic law approximatively above urban canopy (Cheng 2002). It implied that the flow in the roughness sublayer behaved differently above these two different kinds of surfaces. The horizontally-averaged mean velocity profile in the roughness sublayer and inertial sublayer from our research results obeys a single log-law apparently (Fig. 7 (a)). But the zero-plane displacement height z_d and roughness length z_0 regressed by different methods exhibit very large scatter even for similar roughness geometries (Grimmond and Oke 1999). It is suggested that the two-parameter regression that used an appropriate friction velocity U_* was more accurate and generally recommended (Cheng 2002, Kanda 2004). Kanda chose $U_{*z=H}$ which was the frictional velocity at the roof level to regress z_d and z_0. Cheng presented the way that adopted U_* (RS and IS, roughness sublayer and inertial sublayer) which was the spatially averaged shear stresses in the whole surface layer to regress z_d and z_0. Coceal, *et al.* (2006) regressed z_d and z_0 by an effective, spatially-averaged mixing length l_m. The detailed method could be referred to in their paper. This

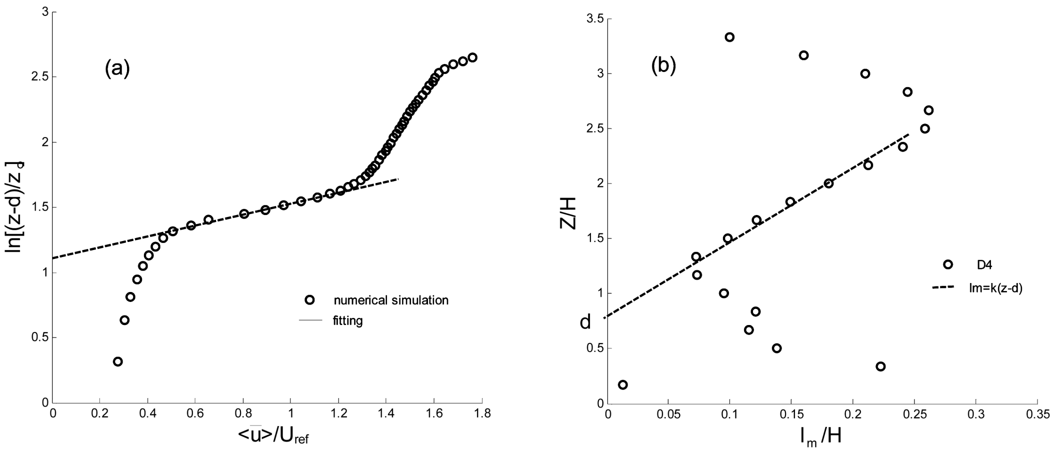

Fig. 7 Horizontally-averaged mean velocity normalized by log law (a) and the effective, spatially-averaged mixing length l_m (b) for D4

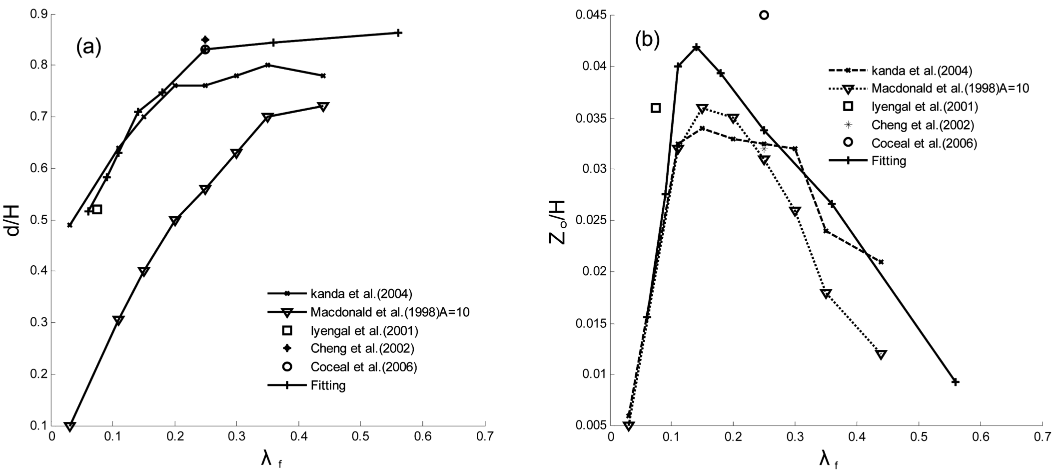

Fig. 8 Zero-plane displacement z_d and Roughness length z_0 versus cube front area density λ_f

paper regressed z_d and z_0 with the method from Coceal (Fig. 7 (b)). Our results and the work of predecessor are shown in Fig. 8. Although the quantities of z_d and z_0 are different because of different methods, the trend of the profiles is similar. z_d heighten with increasing λ_f, whereas z_0 heighten firstly and then lower with increasing λ_f. The maximum of z_0 occurs when λ_f is about 0.14 ("wake interference" flow).

Cheng (2002) proposed that the friction velocity and the roughness length were significantly larger and the "roughness efficiency" was greater for the random surface than for the uniform surface. Macdonald, *et al.* (1997, 2002) proposed that the roughness length z_0 and the zero-plane displacement height z_d for a staggered array were larger than for an aligned array. Grimmond and Oke (1999) also presented that the roughness length for a staggered array was twice as large as an equivalent in line array. However, the value of z_d and z_0 versus σ_h and r_s have not been investigated systematically. The linear expressions about z_d and z_0 versus σ_h and r_s have been obtained on the basis of simulation results (Fig. 9). The expressions are as follow:

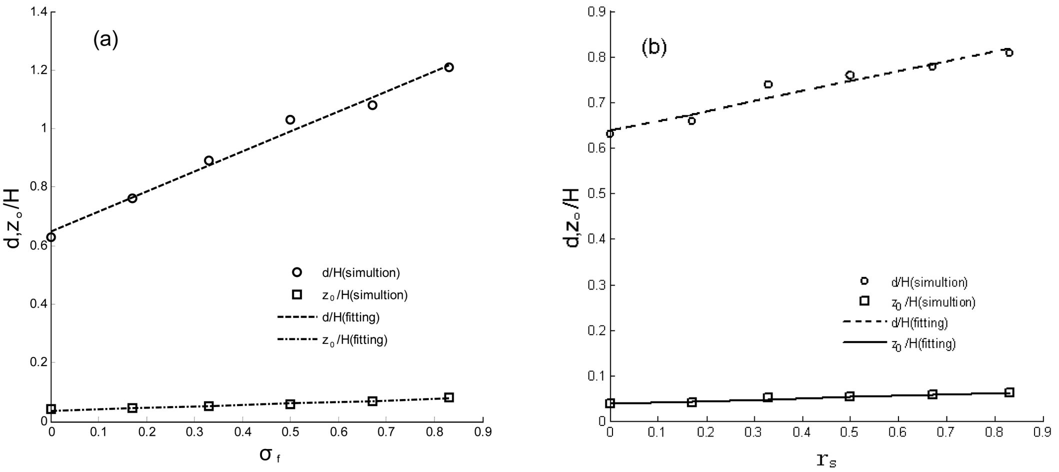

Fig. 9 Linear fitting of zero-plane displacement z_d and roughness length z_0 versus σ_h (a) and r_s (b)

$$z_d = 0.69\sigma_h + z_{dref} \tag{8}$$

$$z_0 = 0.05\sigma_h + z_{0ref} \tag{9}$$

$$z_d = 0.22r_s + z_{dref} \tag{10}$$

$$z_0 = 0.03r_s + z_{0ref} \tag{11}$$

where z_{dref} and z_{0ref} are the reference zero-plane displacement and roughness length of the building arrays whose height is equal and layout is square. z_d and z_0 heighten linearly with σ_h and r_s, If σ_h is large enough, z_d may become higher than the average height of buildings. Whereas, these expressions are summarized from numerical simulation model, and it should be validated by laboratory experiments or field observation which would be the subsequent work for us.

4. Conclusions

Large eddy simulations have been performed within and above three types of urban building arrays to study the systematic role of building spacing, height and layout on mean wind and turbulent characteristics. Some results were achieved by LES:

(1) "Isolated roughness" flow occurs when λ_f is between 0.04 and 0.06, "wake interference" flow occurs when λ_f is between 0.08 and 0.18 and "skimming" flow occurs when λ_f is between 0.25 and 0.56. The shape and structure of vortexes within building arrays would be changed with various σ_h. With increasing σ_h, the wind velocity in the canopy increases and some vortexes in the arrays break, even disappear, whereas other vortexes strengthen and expand. The "street canyon" effect decreases with increasing r_s within the building canopy. If the building arrays are staggered enough, the "street canyon" effect would disappear. (2) The decay of horizontally-averaged mean wind velocity within and above the building arrays is sensitive to λ_f, σ_h and r_s. The wind velocity is positive correlation with λ_f above the building canopy and inverse correlation with λ_f within the building canopy. The wind velocity increases with increasing σ_h within the building canopy, whereas it is just the opposite above the building canopy. The decay of wind velocity increases with

increasing r_s from the ground to 2.5H on the whole. All the wind velocity profiles and the upstream profile converge at the height of 2.5H approximately. Macdonald's model described the wind velocity profiles within the canopy very well for square and staggered building arrays which are not too densely and sparsely packed, but the model should be modified through introducing σ_h for various height building arrays. (3) Vertical profiles of turbulence kinetic energy, TKE, also depends on λ_f, σ_h and r_s. The maximum of TKE always locates at 1.2 times as high as the buildings. TKE decreases with increasing λ_f or r_s within the building canopy because the wind velocity is smaller for dense buildings or stagger buildings. The maximum of TKE are very close though σ_h varies. (4) Temporally- and horizontally-averaged wind velocity profile follows the logarithmic law approximatively above the building canopy. The author regressed z_d and z_0 by an effective mixing length l_m. The results are similar to the work of predecessor for different λ_f. z_d and z_0 heighten linearly with σ_h and r_s.

Finally, some improvements that should be made in further study are discussed. First, the authors considered respectively the influence of various building area density, height fluctuation degree and range staggered degree on airflow and turbulent characteristics, but the distributions of the buildings in the real cities is always random and heterogeneous. It is suggested that integrative effect of λ_f, σ_h and r_s on mean wind and turbulent should be performed for further research. Second, the current study has not referred to the influence of building shape and thermal properties on turbulent statistics. It will be a part of our further research to describe the effect of building shape and thermal properties accurately.

Acknowledgements

This research was supported by the National Natural Science Foundation of China (Grant Numbers: 40333027, 40775014).

References

Belcher, S. E., Jerram, N. and Hunt, J. C. R. (2003), "Adjustment of a turbulent boundary layer to a canopy of roughness elements", *J. Fluid Mech.*, **488**, 369-398.

Cheng, H. and Castro, I. (2002), "Near wall flow over urban-like roughness", *Boundary-Layer Meteorol.*, **104**, 229-259

Cheng, Y., Lien, F. S., Yee, E. and Sinclair, R. (2003), "A comparison of large eddy simulations with a standard k–ε Reynolds-averaged Navier-Stokes Model for the prediction of a fully developed turbulent flow over a matrix of cubes", *J. Wind Eng. Ind. Aerodyn.*, **91**, 1301-1328.

Chu, A. K. M., Kwok, R. C. W. and Yu, K. N. (2005), "Study of pollution dispersion in urban areas using computational fluid dynamics (CFD) and geographic information system (GIS)", *Envir. Mod. And Sofew.* **20**, 273-277.

Coceal. O. and Belcher, S. E. (2004), "A canopy model of mean winds through urban areas", *Q. J. R. Meteorol. Soc.*, **130**, 1349-1372.

Coceal. O. and Belcher, S. E. (2005), "Mean winds through an inhomogeneous urban canopy", *Boundary-Layer Meteorol.* **115**, 47-68.

Coceal. O., Thomas, Y. G., Castro, I. P. and Belcher, S. E. (2006), "Mean flow and turbulence statistics over groups of urban-like cubical obstacles", *Boundary-layer Meteorol.* **121**, 491-519.

Cionco, R. M. (1972), "A wind-profile index for canopy flow", *Boundary-Layer Meteorol.* **3**, 255-263.

Davidson, M. J., Snyder, W. H., Lawson, R. E. and Hunt, J. C. R. (1996), "Wind tunnel simulations of plume dispersion through groups of obstacles", *Atmos. Environ.*, **22**, 3715-3731.

Deardorff, J. W. (1980), "Stratocumulus-topped mixed layers derived from a three-dimensional model", *Boundary-Layer Meteorol.*, **18**, 495-527.

Duijm, N. J. (1999), "Estimates of roughness parameters for arrays of obstacles", *Boundary-Layer Meteorol.*, **91**, 1-22.

Ehrhard, J. and Moussiopoulos, N. (2000), "On a new nonlinear turbulence model for simulating flows around building-shaped structures", *J. Wind Eng. Ind. Aerodyn.*, **88**, 91-99.

Golaz, J. C., Wang, S. Doyle, J. D. and Schimdt, J. (2005), "Coamps-LES: model evaluation and analysis of second-and third-moment vertical velocity budgets", *Bound-Layer Meteorol.*, **116**, 487-517.

Grimmond, C. S. B. and Oke, T. R. (1999), "Aerodynamics properties of urban areas derived from analysis of surface form", *J. Appl. Meteorol.*, **38**, 1262-1292.

Hanna, S. R., Tehranian, S., Carissimo, B., Macdonald, R. W. and Lohner, R. (2002), "Comparisons of model simulations with observations of mean flow and turbulence within simple obstacle arrays", *Atmos. Environ.*, **36**, 5067-5079.

Hunter, L. J., Johnson, G. T. and Watson, I. D. (1992), "An investigation of three-dimensional characteristics of flow regimes within the urban canyon", *Atmos. Environ.*, **20**, 425-432.

Iyengar, A. K. S. and Farell, C. (2001), "Experimental issues in atmospheric boundary layer simulations: Roughness length and integral length scale determination", *J. Wind Eng. Ind. Aerodyn.*, **89**, 1059-1080.

Kanda, M., Moriwaki, R. and Kasamatsu, F. (2004), "Large-eddy simulation of turbulent organized structures within and above explicitly resolved cube arrays", *Boundary-Layer Meteorol.*, **112**, 343-368.

Lien, F. S. and Yee, E. (2004), "Numerical modelling of the turbulent flow developing within and over a 3-D building array, Part I: A high-resolution reynolds-averaged navier-stokes approach", *Boundary-Layer Meorol.*, **112**, 427-466.

Lien, F. S., Yee, E. and Cheng, Y. (2004), "Simulation of mean flow and turbulence over a 2D building array using high-resolution CFD and a Distributed Drag Force Approach", *J. Wind Eng. Ind. Aerodyn.* **92**, 117-158.

Lien, F. S. and Yee, E. (2005), "Numerical modelling of the turbulent flow developing within and over a 3-D building array, Part III: A distributed drag force approach, its implementation and application", *Boundary-Layer Meteorol.*, **114**, 287-313.

Macdonald, R. W., Griffiths, R. F. and Hall, D. J. (1998), "An improved method for the estimation of surface roughness of obstacle arrays", *Atmos. Environ.*, **32**, 1857-1864.

Macdonald, R. W., Griffiths, R. F. and Hall, D. J. (1998), "A comparison of results form scaled field and wind tunnel modelling of dispersion in arrays of obstacles", *Atmos. Environ.*, **32**, 3845-3862.

Macdonald, R. W. (2000), "Modelling the mean velocity profile in the urban canopy layer", *Boundary-Layer Meteorol.* **97**, 25-45.

Macdonald, R. W., Schofield, S. C. and Slawson, P. R. (2002), "Physical modeling of urban roughness using arrays of regular roughness elements", *Water, Air, and Soil Pollution: Focus.*, **2**, 541-554.

Mavroidis, I. and Griffiths, R. F. (2001), "Local characteristics of atmospheric disperion within building arrays", *Atmos. Environ.*, **35**, 2941-2954.

Oke, T. R. (1988), "Street design and urban canopy layer climate", *Energ. Buildings*, **11**, 103-113.

Raupach, M. R., Coppin, P. A. and Legg, B. J. (1986), "Experiments on scalar dispersion within a model plant canopy, Part 1: The turbulence structure", *Boundary-Layer Meteorol.*, **35**, 21-52.

Sada, K. and Sato, A. (2002), "Numerical calculation of flow and stack-gas concentration fluctuation around a cubical building", *Atmos. Environ.*, **36**, 5527-5534.

Snyder, W. H. and Castro, I. P. (2002), "The critical Reynolds number for rough-wall boundary layers", *J. Wind Eng. Ind. Aerodyn.*, **90**, 41-54.

Uehara, K., Wakamatsu, S. and Ooka, R. (2003), "Studies on critical reynolds number indices for wind-tunnel experiments on flow within urban areas", *Boundary-Layer Meteorol.*, **107**, 353-370.

Yee, E. and Biltoft, C. A. (2004), "Concentration fluctuation measurements in a plume dispersing through a regular array of obstacles", *Boundary-Layer Meteorol.*, **111**, 363-415.

Zhang, N. and Jiang, W. M. (2004), "Numerical method study of how buildings affect the flow characteristics of an urban canopy", *Wind Struct.*, **7**, 159-173.

Zhang, N. and Jiang, W. M. (2006), "A large eddy simulation on the effect of buildings on urban flows", *Wind Struct.*, **9**(1), 23-25.

CC